# Microfluidic routing of aqueous and organic flows at high pressures: fabrication and characterization of integrated polymer microvalve elements

Brian J. Kirby,†* David S. Reichmuth, Ronald F. Renzi, Timothy J. Shepodd and Boyd J. Wiedenman

This paper presents the first systematic engineering study of the impact of chemical formulation and surface functionalization on the performace of free-standing microfluidic polymer elements used for high-pressure fluid control in glass microsystems. System design, chemical wet-etch processes, and laser-induced polymerization techniques are described, and parametric studies illustrate the effects of polymer formulation, glass surface modification, and geometric constraints on system performance parameters. In particular, this study shows that highly crosslinked and fluorinated polymers can overcome deficiencies in previously-reported microvalve architectures, particularly limited solvent compatibility. Substrate surface modification is shown effective in reducing the friction of the polymer–glass interface and thereby facilitating valve actuation. A microchip one-way valve constructed using this architecture shows a $2 \times 10^8$ ratio of forward and backward flow rates at 7 MPa. This valve architecture is integrated on chip with minimal dead volumes (70 pl), and should be applicable to systems (including chromatography and chemical synthesis devices) requiring high pressures and solvents of varying polarity.

## Introduction

The ability to control the flow and interaction of fluids is central to increasing the functionality of microfluidic systems. A variety of fluid control techniques has been used for various purposes, including electrokinetic sample injections in miniaturized separation systems,[1] routing of flow through different channels,[2] sealing of reaction zones,[3,4] throttling or metering of flows,[5–9] and high-pressure injections for liquid chromatography systems.[10,11] While external flow control devices have found application for some simple tasks, increasingly sophisticated and sensitive devices have required facile manipulation of smaller and smaller volumes of fluid on-chip.

Crucial applications motivate development of microfluidic valving with the capability to manipulate both aqueous and organic liquids at high pressures (>1 MPa). Increased pressure improves the efficacy of processes that require analyte–surface interactions in porous media, such as chromatography[12,13] or enzymatic reaction,[14,15] since they allow the characteristic pore size to be reduced and the specific surface area increased. In gas-phase systems, increases in pressure also facilitate chemical reactions (*e.g.*, combustion) that are quenched by surface reactions but gain benefit from high analyte density.[16] Compatibility with varying solvents is important for chemical syntheses, which often use harsh solvents; and chromatographic analyses, which typically use varying solvent hydrophobicity or salinity to enable efficient chromatographic separation. Of these, perhaps the clearest area of impact for high-pressure microfluidic valving is in miniaturized high-performance liquid chromatography (HPLC), due to HPLC's ubiquity in chemical analysis systems.

Many significant advances in microfluidic valving have been presented, leading to improvements in the utility of various microfluidic platforms; however, the valve architectures presented to date are unable to control small volumes of both aqueous and organic liquids at pressures typical of flow through porous media (7–40 MPa). Depending on the platform, these limitations are due either to limited mechanical integrity or limited solvent compatibility. Elastomeric substrates, particularly poly(dimethylsiloxane), have been successfully used to develop microvalves using multilayer systems.[4,17] They have been applied primarily to low-pressure aqueous systems due to the limited solvent resistivity[18] and pressure holdoff capacity of elastomeric substrates. Micromachined silicon valves[19,20] are limited in that they are generally unable to hold off >1 MPa pressures, are often incompatible with chemical separation techniques that employ high voltages, and often dissipate substantial power. Hydrogel valves[2,8] have not been employed for flow through porous media since they only offer about an order of magnitude reduction in flow rates and are limited by solvent effects and slow actuation times. Poly(N-isopropylacrylamide) hydrogels have been shown to open and close in response to temperature changes;[21] however, high-pressure holdoff in these systems has been achieved only with 5 mm polymer structures and thus large (>10 nl) dead volumes. Freeze–thaw microvalves using paraffin structures can be heated and cooled to open and close microfluidic pathways,[7] however, they have not been shown to hold off high pressure and the paraffins can be dissolved by organic solvents.

Mobile free-standing polymer microvalves[9–11] have been used as a straightforward and inexpensive means to address, among other issues, the challenge of controlling

† Current address: Sibley School of Mechanical and Aerospace Engineering, Cornell University, Ithaca, NY 14853, USA.
*bk88@cornell.edu

high-pressure-driven flow on chip. The motion of free-standing polymer elements[9,10] can be used for a variety of flow control functions on microchips. Polymer elements may be fabricated *in-situ* and engineered to slide easily along microchannels, controlling flow pathways *via* face seals formed against the substrate. Such systems have been used to hold off pressures as high as 50 MPa.[10]

Here, we present a systematic study of the effects of polymer crosslinking and fluorination as well as substrate functionalization on microsystem performance with attention to attributes required for successful operation of valves at high pressure with both aqueous and organic liquids. Using a polymer formulation inspired by this study, we demonstrate a high-pressure one-way microvalve that operates in both water and acetonitrile.

## Techniques

**System conceptual design.** The microvalve architecture discussed here uses the motion of a polymer element within a three-dimensional microfluidic structure to control fluid flow.[9–11] Pressure differentials result in the opening and closing of fluidic pathways in the chip as the polymer element forms face seals with the silica substrate (Fig. 1).

Devices are fabricated using a combination of chemical wet-etching of silica wafers and *in-situ* photopatterning of polymer monoliths (Fig. 1a).[9–11] The glass substrate forms microchannels for fluid flow as well as an area in which the polymer element will be fabricated. The photopatterned polymer element is a free-standing flexible element that is shaped to match the channel dimensions, but can move to open and close fluid pathways through face seals against the silica microchannels.

The devices described here have two separately-etched levels, one deep ($\sim 20$ μm) and one shallow ($\sim 5$ μm). In contrast to typical microchip fabrication procedures, both glass substrates (base and cover) are etched. The base substrate contains the majority of the microfluidic channels; however, the cover substrate is etched with a mirror image of the base wafer pattern in the region where the polymer element is to be fabricated. Base and cover wafers are aligned (typically to within 3–5 μm) and bonded. This design leads to a roughly isotropic constriction at the edge of the doubly-etched region that leads to a robust valve seat. The three-dimensional structure generated by this etch process leads to a nearly cylindrical microchannel geometry (45 μm width, 40 μm depth) and a nearly cylindrical polymer element, which forms a face seal against a shallow channel (15 μm width, 5 μm depth) generated by the shallow etch.

**Wafer fabrication.** Data presented here is taken from experiments on valve systems on both fused silica and borosilicate glass substrates. No performance difference could be observed between valve systems fabricated in fused silica and borosilicate glass substrates; therefore, no distinction will be made in the Results or Discussion section regarding the particular glass or silica type.

Silica microchips were fabricated from Corning 7980 fused silica wafers of 100 mm diameter and 0.75 mm thickness (Sensor Prep Services, Inc., Elburn, IL) using standard photolithography, wet etch, and bonding techniques. Photomasks were designed using CleWin (WieWeb software, The Netherlands), and chromium-on-glass photomasks were generated by PhotoSciences (San Jose, CA). 150 μm diameter access holes were drilled in the cover plate (Corning 7980) with diamond-tipped
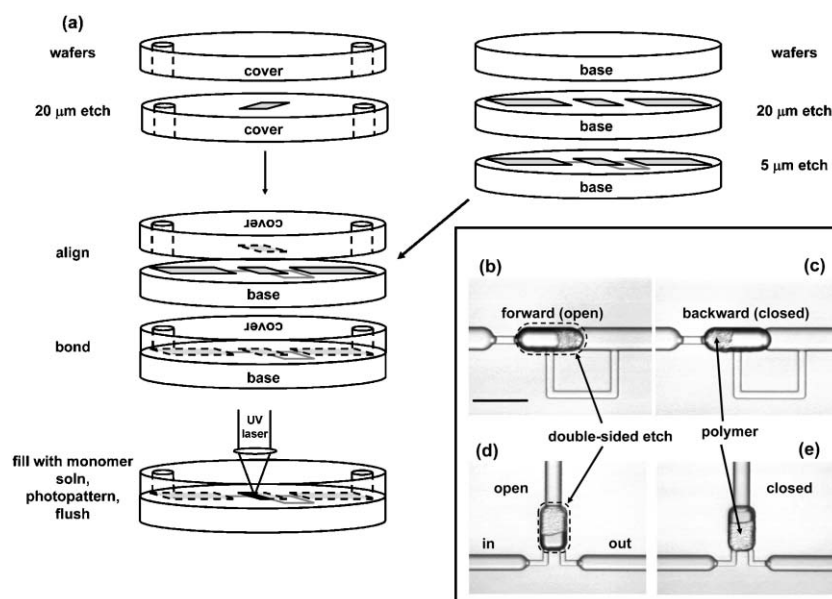


**Fig. 1** Fabrication of silica microchannels and *in-situ* laser-polymerized polymer element. (a): fabrication involves 20 μm and 5 μm isotropic wet etch steps. The area in which the polymer is to be constructed is etched into both base and cover wafers. Shaped UV laser light patterns the polymer in place. (b)–(c): a one-way valve (scale bar = 100 μm). (b): pressure at left causes the polymer to seat to the right, allowing fluid through the bypass. (c): pressure at right causes the polymer to seat to the left, closing off fluid flow. (d)–(e): on/off valve. (d): with no pressure at the control line at top, the polymer stays at top and flow moves from inlet to outlet. (e): with pressure applied at top, the fluidic pathway is closed and flow stops.

drill bits (Amplex, Worcester, MA) before all cleanroom steps.

The fused silica etch process is as follows: the hard mask was generated through LPCVD deposition of a 150 nm amorphous silicon layer. A 7.5 μm-thick layer of SJR 5740 (Shipley Corporation, Marlborough, MA) positive photoresist was spin-coated and soft-baked (90 °C, 5 min). The mask pattern was transferred to the photoresist by exposing it to UV light in a contact mask aligner (MA6, Karl Suss America Inc., Waterbury Center, VA) at 775 mJ cm$^{-2}$. Exposure time varied depending on flux intensity. After exposure, the photoresist was developed with Microposit developer (Shipley Corporation, Marlborough, MA) and hard-baked (125 °C, 30 min). Exposed silicon was etched in an Oxford (Yatton/Bristol, UK) Plasma Lab 100, 13.56 MHz driven parallel plate reactor, using a 30 s oxygen ash @ 50W DC & 50 mTorr, followed by a 150 s SF$_6$ plasma treatment at 200W DC, 50 mTorr. The subsequently exposed silica was etched at a 1.2 μm min$^{-1}$ nominal etch rate with a 49% HF solution (Shape Products Company, Oakland, CA). Following the silica etch step, wafers were cleaned in acetone followed by a piranha-etch solution (4 : 1 H$_2$SO$_4$ : H$_2$O$_2$, 100 °C). The surfaces were treated in 40% w/w NaOH (80 °C), rinsed and dried. Following etch steps, the bottom and cover wafers are aligned to a precision of 3–5 μm using the mask aligner and are thermally bonded for 5 h at 1150 °C in an N$_2$-purged programmable furnace (Thermolyne, Dubuque, IA).

Glass wafers were fabricated using essentially similar techniques, with the following differences: (1) Schott D263 borosilicate glass wafers were used (100 mm diameter, 1.1 mm thickness, S. I. Howard Glass Company, Worcester, MA); (2) sputtered 200 nm chromium layers were used as a hard mask; (3) exposed chrome was etched with CEN 300 Micro-chrome etchant (Microchrome Technologies Inc., San Jose, CA); (4) exposed glass was etched with a 16% HF solution (Shape Products Company, Oakland, CA) at a nominal etch rate of 2.0 μm min$^{-1}$; and (5) wafers were bonded at 610 °C.

**Fluidic handling.** Fluids were introduced on-chip both for fabrication (microvalve patterning and surface modification) and for valve performance characterization. A number of fluidic handling techniques were developed to enable high-pressure connections of capillary systems to chip for testing and evaluation at high pressure. In all cases, 360 μm OD capillaries (silica, polyetheretherketone (PEEK), or stainless steel) were inserted into custom-machined, one-piece sleeveless PEEK male ferrules (Fig. 2a). Female ports (Fig. 2b) were machined from PEEK or polyetherimide (ULTEM) rod stock (McMaster-Carr, Santa Fe Springs, CA). Hand- or tool-tightening the fitting swages the ferrule around the capillary to create a seal that holds liquids at pressures up to 35 MPa or 70 MPa, respectively. For coating techniques and initial polymer fabrication steps that required only subatmospheric pressure differentials, fluids were introduced by filling
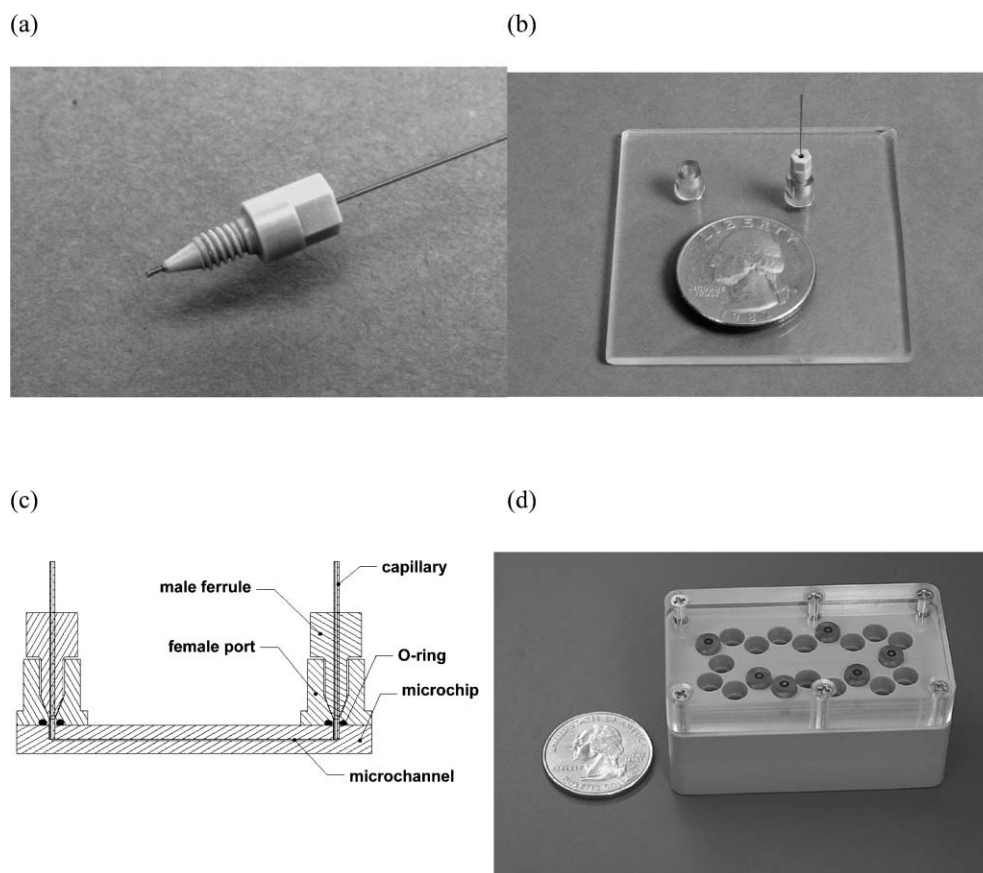


(a)

(b)

(c)

(d)

**Fig. 2** High-pressure fluidic connections. (a) Male ferrule and capillary. (b) Female ports bonded to glass wafer. (c) Side cross-sectional schematic of bonded fittings and seals. (d) Alignment jig for attaching permanent epoxied fitting with O-ring seal.

reservoirs and then manipulated using capillary action or application of vacuum to various ports.

Permanent high-pressure connections were realized with epoxy-bonded ULTEM ports (Fig. 2b), which provided high pressure holdoff (8.5 MPa) and robust performance. The silicone or Buna-N O-ring in each ULTEM port both maximized yield by keeping epoxy out of the microchannel to prevent clogging and kept system solvents separate from the epoxy to ensure reliable bonding. An alignment jig (Fig. 2d) matching the standard hole pattern on the microchip positioned the ULTEM ports during epoxy application and secured the system in compression during bonding and curing. The compression simultaneously optimized the mechanical integrity of the epoxy seal and ensured that O-rings were permanently held in their compressed state.

**Polymer synthesis.** All chemicals used for polymer synthesis were obtained from Sigma-Aldrich (St. Louis, MO) and used as received, unless otherwise specified. These included but were not limited to 2, 2′-azobisisobutyronitrile (AIBN), pentaerythritol triacrylate (PE3), pentaerythritol tetraacrylate (PE4), ethyl acrylate (EA), 2,2,2-trifluoroethyl acrylate (3FEA), propyl acrylate (PA), 2,2,3,3,3-pentafluoropropyl acrylate (5FPA), butyl acrylate (BA), 2,2,3,4,4,4-hexafluorobutyl acrylate (6FBA), and 2,2,3,3,4,4,4-heptafluorobutyl acrylate (7FBA). 2,2,3,3-Tetrafluorobutanediol diacrylate (TF-BDDA) was obtained from Monomer-Polymer & Dajac Laboratories (Feasterville, PA). Fluorinert® FC-84 (FC84) was obtained from 3M (St. Paul, MN). Tridecafluoro-1,1,2,2-tetrahydrooctyltriethoxysilane (TDFTES) was obtained from Gelest, Inc. (Tullytown, PA). All formula ratios are by volume unless specified otherwise.

Patterning of polymer elements *in-situ* was achieved using local photoinitiation of radical species through adsorption of 355 nm light by an azo initiator (AIBN). The output of a passively Q-switched, frequency-tripled Nd : YAG laser (12 kHz, 4 mW, 355 nm; Nanolase, JDS Uniphase, San Jose, CA) was projected through an adjustable slit and focused onto a microchannel filled with monomer solution to create a solid polymer element. Since the polymer elements were cast in-place, the element cross-section conformed to the microchannel geometry (20–100 μm diameter), while the length of the polymer element (40–150 μm) was controlled by controlling the magnification of the projection optics and the width of the slit. Polymerization occurred after 20–90 s of exposure, monitored using video microscopy. After polymerization, the chip was flushed with acetonitrile to remove residual monomer.

**Microchannel surface modification.** For some experiments, the glass or silica substrate was modified to minimize the friction coefficient observed by the mobile polymer element. Coating was achieved by incubating microchannel surfaces with a solution of 1,4-dioxane, glacial acetic acid, TDFTES, and water in a 30 : 5 : 4 : 1 ratio at 70 °C for various lengths of time, during which hydrolysis and condensation of the ethoxysilane groups with the glass/silica wall leads to functionalization of the surface with tridecafluorooctyl ($C_8H_4F_{13}$) groups.

**Materials and performance characterization.** A number of procedures were used to characterize the properties of the polymer elements and microvalve systems described here. Polymer actuation pressure was characterized in silica capillaries or microchannels *via* microscope observation while slowly increasing pressure was applied and monitored *via* a strain-gauge pressure transducer (Senso-Metrics SP-70D, Simi Valley, CA). Valve sealing performance was evaluated on-chip by measuring flow rates *vs.* pressure with valves open and closed. Flow rate was evaluated either by observation of a moving meniscus in transmission or epifluorescent imaging of moving dye fronts combined with inversion of scalar advection–diffusion equations. The responses of the size of the valve elements to changes in solvent were measured through microscope observation while valve elements were exposed to a variety of solvents. Solubility was monitored by storing polymer elements overnight in a variety of solvents and observing any effects on the polymer.

## Results and discussion

Measurements of key performance parameters of the fabrication technique, polymer elements, and the resulting microvalve systems were used to (1) show the influence of substrate functionalization and (2) demonstrate the ability of mobile polymer monolith architectures to provide fluidic control in high-pressure flows with a variety of solvents. These measurements are discussed in the following sections.

### Actuation pressure and solvent-induced expansion and contraction

The polymer elements described here are actuated by pressure differentials in their microfluidic system, and are exposed to widely varying solvents during operation. Because of this, optimal performance requires that the polymer elements actuate at low pressure and show chemical and mechanical insensitivity to a wide range of solvent. The effects of various design inputs on performance in these areas is presented in the following paragraphs.

Simple phenomenological tribological relations can be used to illustrate the scaling relations that describe actuation pressure as well as the parametric inputs that can be used to minimize it. By postulating a pressure $P_{int}$ internal to the monolith and a static friction coefficient $c_f$ at the polymer–substrate interface, a simple relation describing the actuation pressure for a cylindrical element can be derived from the definition of friction coefficient:

$$P_{act} = c_f P_{int} \frac{4\ell}{d} \qquad (1)$$

where $\ell$ is the cylinder length, $d$ is the cylinder diameter, and $P_{act}$ is the pressure required to actuate the element. This relation illustrates the expected dependence of the required actuation pressure on the polymer length and polymer diameter as well as friction coefficient and internal pressure.

Directed experiments have been used to confirm the parametric dependences in eqn. (1) and illustrate techniques for minimizing the pressure required to mobilize the polymer elements. Since length and diameter can be varied directly,

measurements as a function of geometry have been used to confirm their scaling in eqn. (1). Since friction coefficient and internal pressure cannot be varied directly, the effects of variations in polymer formulations and surface treatments have been measured in an attempt to demonstrate optimal actuation pressure performance.

Eqn. (1) illustrates that the size of these polymer elements may be scaled arbitrarily at constant aspect ratio without affecting the pressure required to actuate them. This can be inferred from observations that actuation pressure varies linearly with polymer length and inversely with polymer diameter (Fig. 3). The actuation pressure is constant at constant aspect ratio $\ell/d$, since these effects cancel.

Surface chemistry can be used to minimize the actuation pressure by minimizing the friction coefficient in eqn. (1). Hydrolysis and condensation of fluoroalkyl alkoxysilanes at the glass surface can be used to reduce the surface energy of the glass surface and thereby reduce the observed friction coefficient of the wall–polymer interface. Incubation to modify the substrate surface with tridecafluorooctyl groups (see Experimental section for details) reduces the actuation pressure by approximately a factor of 6 (Fig. 4).

The chemical formulation of the polymer element affects the polymer's surface energy, pore structure, mechanical strength, and solvent affinity; these, in turn, influence the observed friction coefficient and solvent-induced expansion and contraction. In general, acrylate polymers are hydrophobic and contract when exposed to aqueous solutions. Polymer contraction and incompatibility with aqueous solvents is the primary limitation in the valve systems presented in refs. 9 and 10.

Characterization of polymer elements constructed from varying monomer solutions were used to explore the effects of chemical composition on element performance. Two systematic studies were performed to elucidate, in turn, the parametric effects of (1) polymer cross-linking density and (2) fluorination of pendant alkyl groups on actuation pressure and solvent interaction performance. Polymer cylinders with varying monomer/solvent formulations were fabricated in capillaries or microchannels. The pressures required to actuate the polymer elements were recorded, and, since the effects of geometry are well-understood (eqn. (1) and Fig. 3), the actuation pressure was normalized by the aspect ratio $\ell/d$. Following actuation, the polymer elements were flushed extensively with acetonitrile, and exposed sequentially to acetonitrile and water. These two solvents were chosen since they are the primary constituents of most high-pressure liquid chromatography separation buffers and because they represent the two extremes of hydrophilicity these microvalve systems will likely face when used in that capacity. Changes in the size of the polymer element during sequential immersion in acetonitrile and water were recorded. Normalized actuation pressure ($P^* = P_{act}d/\ell$) is then plotted as a function of the ratio of monolith lengths in water and acetonitrile ($\gamma = \ell_{water}/\ell_{ACN}$) in Figs. 5 and 6, with normalized pressure *decreasing* along the ordinate. This style of plotting the data illustrates the tradeoffs
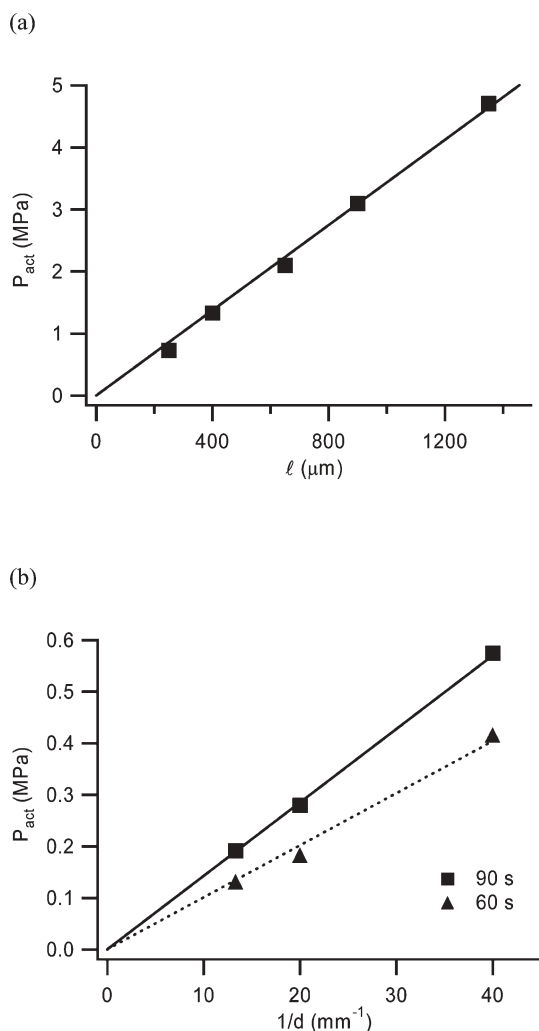
(a)

(b)

**Fig. 3** Actuation pressure as a function of (a) polymer length and (b) diameter. Polymer formulation: 3 : 3 : 4 ratio of 1,3-butanediol diacrylate, 3FEA, and 1-propanol. (a): 75 µm diameter polymer elements in untreated fused silica capillaries. (b) 100 µm long polymer elements in untreated silica capillaries at two exposure times.
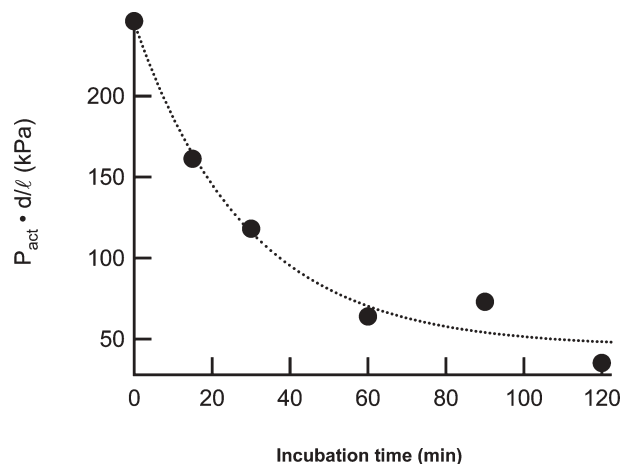
**Fig. 4** Actuation pressure as a function of incubation time with fluoroalkyl coating. Substrate: fused silica capillaries. Polymer formulation: 5 : 5 : 3 : 3 ratio of TF-BDDA, 7FBA, 3FEA, and FC-84; photoinitiated with 10 mg ml$^{-1}$ of AIBN. Dashed line is exponential fit to data.
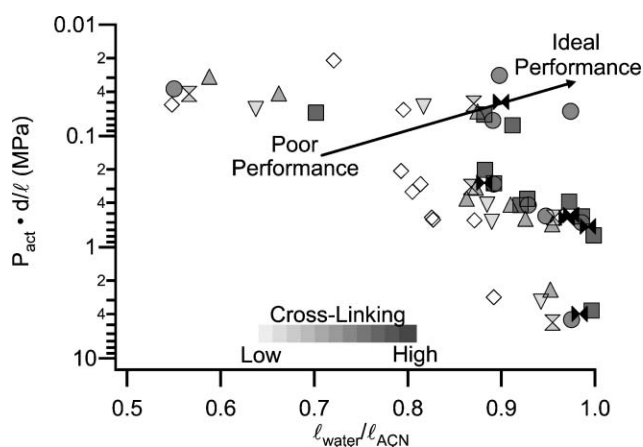
**Fig. 5** Increased crosslinking density improves the actuation pressure–solvent insensitivity performance of cylindrical polymer elements in silica microchannels or capillaries. Note: values on the $y$-axis decrease with height. Ideal performance at top right corresponds to solvent-resistance and low-pressure actuation. Darkness of symbols is qualitatively proportional to C=C double bond concentration in the monomer/solvent solution. Data shown for the following crosslinker fractions: diamonds: 20% PE3; down triangles: 40% PE3; up triangles: 60% PE3; circles: 80% PE3; squares: 100% PE3; vertical bowtie: 60% PE4; standard bowtie: 100% PE4. Remaining monomer (if any) is butyl acrylate in all cases.
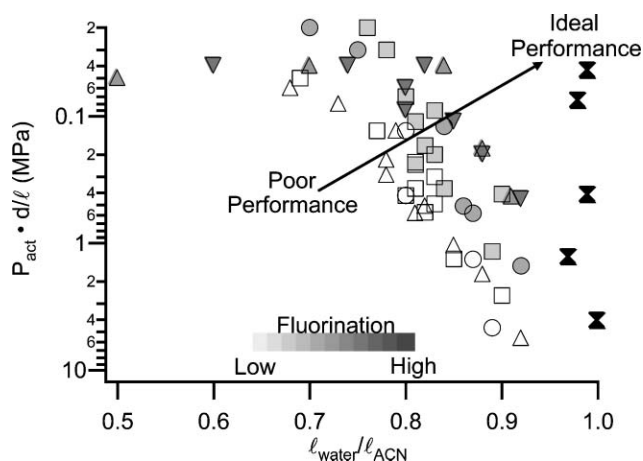


**Fig. 6** Fluorination improves the actuation pressure–solvent insensitivity performance of cylindrical polymer elements in silica microchannels or capillaries. Note: values on the $y$-axis decrease with height. Darkness of symbols is qualitatively proportional to ratio of C–F to C–H bonds in resulting polymer. All polymers (except bowtie symbols) fabricated from 60 : 40 monomer : solvent solutions, where the solvent is 1-propanol and the monomer is 50% crosslinker (1,3-butanediol diacrylate) and 50% RCOCHCH$_2$. Squares: R=C$_2$H$_5$ (open) or C$_2$H$_2$F$_3$ (shaded). Circles: R=C$_3$H$_7$ (open) or C$_3$H$_2$F$_5$ (shaded). Triangles: R=C$_4$H$_9$ (open), C$_4$H$_3$F$_6$ (shaded, up-facing), or C$_4$H$_2$F$_7$(shaded, down-facing). Bowtie symbols correspond to the formulation specified in Fig. 4.

associated with varying degrees of polymerization and highlights the effects of compositional changes. As illumination time (or laser intensity) is increased, the extent of polymerization increases. Increased polymerization increases the

monolith's mechanical integrity, and thus reduces the degree to which the monolith expands and contracts in response to immersion in solvents for which it has varying affinity. Increased polymerization, however, also increases the pressure required to actuate the polymer element (Fig. 3b). If changes in properties based on polymerization extent are viewed as a curve through $\gamma$–$P^*$ space, compositional changes affect the path that curve takes from upper left (weakly polymerized) to lower right (fully polymerized). Each curve allows the user to design polymer mechanical strength to the desired application, depending on whether hard (fully polymerized) or soft (partially polymerized) polymers are desired. Typically, optimal valve system performance is achieved at design points near the upper-right of this type of graph, where the actuation pressure is low and the size change response to solvent changes is minimal; performance improvements thus occur when the path of the curve is pushed toward the upper-right by compositional changes and their influence on mechanical properties, solvent affinity, or surface chemistry.

The first study shows how increased cross-linking density leads to polymer elements whose increased mechanical strength results in lower actuation pressure for a given size change. Fig. 5 shows results for butyl acrylate monomers crosslinked with varying amounts of pentaerythritol triacrylate (PE3) and pentaerythritol tetraacrylate (PE4). The curves show similar form for all of the tested formulations: (1) at very low laser exposure, the polymer elements are not fully formed, the actuation pressure is immeasurably low (pressure uncertainty of these measurements is approximately 70 kPa), and the low degree of polymerization leads to weak, gel-like polymers that expand and contract greatly (*i.e.*, $\ell_{water}/\ell_{ACN}$ is low); (2) when the polymer is fully formed, the actuation pressure increases dramatically as the solvent-related size changes diminish (*i.e.*, $\ell_{water}/\ell_{ACN}$ moves toward unity). The effect of cross-linking is seen in the shift of the curves to the right. From a design standpoint, this implies that increased cross-linking will either reduce size change effects for a given $P_{act}$ requirement, or reduce $P_{act}$ for a given size change requirement.

The second study shows how fluorination leads to polymer elements whose decreased surface energy leads to lower actuation pressure for a given size change. Fig. 6 shows results for varying monomers crosslinked with 1,3-butanediol diacrylate. Both the length of the pendant alkyl chain of the acrylate monomer and the degree of fluorination of the alkyl chain are varied. The curves again show similar form compared to each other and to the curves in Fig. 5. The effect of fluorination is seen in the shift of the curves up and to the right. Since preliminary evidence on bulk samples (data not shown) indicates that mechanical strength is not significantly changed by fluorination, the reduction (up to $\sim$8-fold) of actuation pressure for fluoroalkyl acrylates as compared to alkyl acrylates are indicative primarily of friction coefficient reduction. Here, the polymer chemistry mimics the low surface energy (albeit not the polymer chain structure) of low-friction polymers such as Teflon.

Fluorination can be added to the solvent as well; in fact, the most successful formulation to date incorporates fluorinated monomers and crosslinkers with a perfluorinated solvent

(Fluorinert℗ FC-84). The presence of the FC-84 and the extensive fluorination of this material limit solvent interaction and lead to polymer elements that show minimal size change upon changes in solvent (see bowtie symbols in Fig. 6).

**Flow control in high-pressure systems**

The dramatic improvements in solvent applicability illustrated in Fig. 6 enable development of high-pressure microfluidic control elements usable in solvents showing a wide range of polarities and thus applicable to a wide range of high-pressure analyses and syntheses. These polymers have been tested for chemical resistance with water, $C_1$–$C_3$ alcohols, THF, acetonitrile, acetone, and fluorinated ion-pairing HPLC reagents (trifluoroacetic acid and heptafluorobutanoic acid). This performance (Fig. 7) has been quantified for a one-way valve (similar to that shown in Fig. 1b and 1c) constructed from highly-crosslinked acrylate. In the case of the one-way valve, flow rates measured in the forward (open) and backward (closed) directions with water or acetonitrile as the working fluid show that the valve effectively allows only forward flow—the ratio of open to closed flow rates in this case is approximately $2 \times 10^8$, and the reverse flow rate is on the order of 1 pl s$^{-1}$ at 5 MPa (Fig. 7). Such operation in water is not possible with previously-reported polymer formulations,[9,10] which would contract in water and fail to seal. Reproducibility and lifetime of these materials is presented in ref. 11.

## Conclusions

A systematic study of the effect of monomer formulation on component-level performance of high-pressure polymer microfluidic control elements has been presented. Actuation performance and chemical and mechanical compatibility with solvents of varying polarity are affected by the choice of monomers and cross-linkers, cross-linking density, and substrate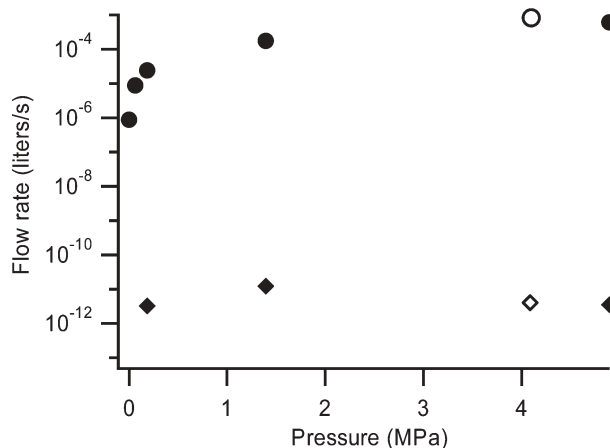 functionalization. Fluorination of pendant alkyl groups in monomers and organosilane-functionalized glass surfaces lead to 8-fold and 6-fold reduction in the pressure required to actuate polymer elements. Increasing the volume fraction of crosslinker from 20% to 100% reduces solvent-induced contraction by a factor of 2–4. A highly-crosslinked material was used to demonstrate a microchip one-way valve with a $2 \times 10^8$-fold reduction in flow rate when closed. Optimal performance involves fluorination of monomers, cross-linkers, solvents, and silica surfaces. These developments enable high-pressure microfluidic control schemes with broad applicability.

**Brian J. Kirby,†\* David S. Reichmuth, Ronald F. Renzi, Timothy J. Shepodd and Boyd J. Wiedenman**
*Sandia National Laboratories, Livermore, CA 94551, USA.*
*E-mail: bk88@cornell.edu*

## References

1 D. Harrison, A. Manz, Z. Fan, H. Ludi and H. Windmer, *Anal. Chem.*, 1992, **64**, 1926.
2 D. J. Beebe, J. S. Moore, J. M. Bauer, Q. Yu, R. H. Liu, C. Devadoss and B. H. Jo, *Nature*, 2000, **404**, 588.
3 C. L. Hansen, E. Skordalakes, J. M. Berger and S. R. Quake, *Proc. Natl. Acad. Sci. USA*, 2002, **24**, 16531.
4 T. Thorsen, S. J. Maerkl and S. R. Quake, *Science*, 2002, **18**, 580.
5 E. T. Carlen and C. H. Mastrangelo, *J. Microelectromech. Syst.*, 2002, **11**, 408.
6 C. A. Rich and K. D. Wise, *J. Microelectromech. Syst.*, 2003, **12**, 201.
7 P. Selvaganapathy, E. T. Carlen and C. H. Mastrangelo, *Sens. Actuators A: Physical*, 2003, **15**, 275.
8 R. H. Liu, Q. Yu and D. J. Beebe, *J. Microelectromech. Syst.*, 2002, **11**, 45.
9 B. J. Kirby, T. J. Shepodd and E. F. Hasselbrink, *J. Chromatogr. A*, 2002, **6**, 1.
10 E. F. Hasselbrink, T. J. Shepodd and J. E. Rehm, *Anal. Chem.*, 2002, **1**, 4913–4918.
11 D. S. Reichmuth, T. J. Shepodd and B. J. Kirby, *Anal. Chem.*, 2004, **76**, 5063–5068.
12 L. R. Snyder, J. W. Dolan and J. R. Gant, *J. Chromatogr.*, 1979, **165**, 3.
13 M. P. Washburn, D. Wolters and J. R. Yates, *Nat. Biotechnol.*, 2001, **19**, 242.
14 M. W. Losey, R. J. Jackman, S. L. Firebaugh, M. A. Schmidt and K. F. Jensen, *J. Microelectromech. Syst.*, 2002, **11**, 709.
15 L. R. Arana, S. B. Schaevitz, A. J. Franz, M. A. Schmidt and K. F. Jensen, *J. Microelectromech. Syst.*, 2003, **12**, 600.
16 I. Glassman, *Combustion*, Academic Press, San Diego, 1996.
17 M. A. Unger, H. P. Chou, T. Thorsen, A. Scherer and S. R. Quake, *Science*, 2000, **288**, 113.
18 J. N. Lee, C. Park and G. M. Whitesides, *Anal. Chem.*, 2003, **75**, 6544.
19 S. Shoji and M. Esashi, *J. Micromech. Microeng.*, 1994, **4**, 157.
20 M. Hu, H. Du, S.-F. Ling, Y. Fu, Q. Chen, L. Chow and B. Li, *J. Micromech. Microeng.*, 2004, **14**, 382.
21 Q. Luo, S. Mutlu, Y. B. Gianchandani, F. Svec and J. M. J. Frechet, *Electrophoresis*, 2003, **24**, 3694.

**Fig. 7** Reverse flow rates through a microchip check valve can be reduced by a factor of $2 \times 10^8$ as compared to forward flow rate. Circles: forward flow rate. Diamonds: leak rate backwards through closed valve. Valve geometry shown in Fig. 1. Working fluid: water (filled symbols) or acetonitrile (open symbols). Polymer composition: 2 : 1 w/w PE3 : 1-propanol photoinitiated by 10 mg ml$^{-1}$ AIBN.